Supporting Information

Broder et al. 10.1073/pnas.1305464110

SI Materials and Methods

Protein Expression and Purification. Recombinant human meprin α and meprin β were expressed in baculovirus-infected insect cells and purified and activated as described previously (1, 2). Full-length human bone morphogenetic protein-1 (BMP-1)-FLAG and recombinant human procollagen C-proteinase enhancer-1 (PCPE-1) with an eight-histidine C-terminal tag were expressed in HEK 293-EBNA cells, then purified as described previously (3). Human matrix metalloproteinase-1 (MMP-1) was expressed in CHO cells and purified to homogeneity as described previously(4).

Purification of Human Procollagen I Heterotrimer. Recombinant human procollagen I heterotrimer was purified from yeast cells (*Pichia pastoris*), kindly supplied by Fibrogen. First, cells were lysed in 0.1 M Tris·HCl and 0.4 M NaCl (pH 7.4) containing protease inhibitors, using glass beads (Biospec Products). After filtration through gaze and centrifugation (15,000 × *g* for 30 min at 4 °C), the supernatant was collected, and high molecular weight proteins were precipitated by addition of PEG 4000 to a final concentration of 5% (wt/vol). After further centrifugation (15,000 × g for 30 min), the supernatant was removed, and the pellet was washed twice in 10 mM Tris·HCl (pH 7.4) containing protease inhibitors. The pellet was then solubilized in 0.1 M Tris·HCl and 0.4 M NaCl (pH 7.4) and clarified by further centrifugation (20,000 × *g* for 60 min). Further purification was provided by heparin-Sepharose affinity chromatography, followed by gel filtration chromatography on a Sephacryl S-500 (GE Healthcare).

Cleavage of Human Procollagen I Heterotrimer and Miniprocollagen α1(I) Homotrimer by Meprin α, Meprin β, and BMP-1/PCPE-1 and Edman Degradation. First, 40 nM human procollagen I heterotrimer or miniprocollagen α1(I) homotrimer (R&D Systems) was incubated with 0.3 nM recombinant proteinase in a total volume of 50 μL for 1, 10, 30, 60, or 90 min at 37 °C in reaction buffer [20 mM Hepes (pH 7.4) for meprin α and meprin β and 50 mM Tris (pH 7.4), 150 mM NaCl, 5 mM $CaCl_2$, and 0.02% Brij35 for BMP-1/PCPE-1]. In the case of BMP-1, PCPE-1 was present at equimolar concentrations with respect to the substrate. Proteins were separated by SDS/PAGE. For N-terminal sequencing, proteins were blotted onto a PVDF membrane, stained with Coomassie brilliant blue, and sequenced at the protein microsequencing center of the Unité Mixte de Service 3444 in Lyon, France.

MS-Based Identification of Meprin Cleavage Sites in Human Procollagen α1(I) and α2(I). Meprin α and meprin β cleavage sites at the amino terminus of mature collagen I heterotrimers were identified by in-gel cyanogen bromide cleavage of the protein and subsequent LC-MS/MS analysis on an Orbitrap Velos mass spectrometer. Identification of C-propeptide cleavage sites was performed by determination of the N-termini of the released C-propeptides, performed in gel by reductive dimethylation and tryptic digestion of the peptides.

Determination of Meprin Cleavage Sites at the N-Propeptide of Procollagen I. Coomassie blue-stained protein bands (Fig. S1*A*) were excised from the acrylamide gel, cut into ∼2-mm cubes, and destained with 50 mM Hepes (pH 8.0), followed by 50 mM Hepes (pH 8.0) in 30% (vol/vol) acetonitrile (ACN). Proteins were reduced using 10 mM DTT and alkylated using 55 mM iodoacetamide in 100 mM Hepes (pH 8.0), after which 10 μL of 25.5 mg/mL cyanogen bromide in 50% formic acid (FA) was added to the gel pieces at 4 °C. Once swelling of the gel pieces was noted, more 50% FA was added to fully cover the gel slices during overnight digestion at 4 °C. After digestion, samples were diluted to 4% FA, and peptides were extracted from the gel with 1% FA in 50% (vol/vol) ACN and 100% ACN with sonication, respectively. The extracted peptides were lyophilized and resuspended in 0.1% TFA and frozen before analysis.

Determination of C-Propeptide Cleavage Sites. Gel pieces were excised and destained (Fig. S1*A*), and proteins were reduced and alkylated. In-gel dimethylation was performed overnight at 37 °C with 30 mM formaldehyde and 15 mM sodium cyanoborohydride in 100 mM Hepes (pH 7.0). The reaction was quenched with 100 mM ammonium bicarbonate for 2 h with shaking. Gel pieces were washed, dehydrated with ACN, and dried by vacuum centrifugation before digestion with 50 ng of trypsin [25 mM Hepes, 5% (vol/vol) ACN] at 37 °C overnight. Peptides were extracted from the gel pieces with 1% FA in 50% (vol/vol) CAN and 100% ACN with sonication, respectively. Samples were reduced in volume using a vacuum centrifuge and filled to equal volumes with 0.1% TFA.

LC-MS. Nano-HPLC-MS was performed on an UltiMate 3000 RS Nano/Cap System (Dionex) coupled online to an Orbitrap LTQ Velos (Thermo Scientific). Samples were desalted for 6 min (Acclaim PepMap100 C-18; 300 μm i.d. × 5 mm, 5 μm, 100 Å) at a flow rate of 30 μL/min using 3% ACN and 0.1% TFA. An Acclaim PepMap100 C-18 column (75 μm i.d. × 150 mm, 3 μm, 100 Å) was used for analytical separation at a flow rate of 300 nL/min using eluent A (0.05% FA) and eluent B (80% ACN and 0.04% FA). Separation was performed using linear gradient steps of 5–12% eluent B (6–7 min), 7–55% eluent B (7–52 min), and 55–95% eluent B (52–55 min), followed by an isocratic wash step (95% eluent B; 55–65 min) and column reequilibration (5% eluent B; 65–80 min).

MS scans were acquired in the range of 300–2,000 *m/z* at a resolution of 60,000. The five most intense signals were subjected to collision-induced dissociation (CID) and higher-energy C-trap dissociation (HCD) fragmentation using a dynamic exclusion of 20 s. MS/MS parameters were chosen as follows: minimum signal intensity of 1,000, isolation width of 3.0 Da, charge state ≥2, HCD resolution 7,500, and normalized collision energy of 35 for CID and 40 for HCD. Lock mass (371.10123) was used for recalibration of data acquired in fragmentation mode.

Data Interpretation. HCD and CID tandem mass spectrometry (MS^2) spectra were exported to separate. mgf files using Proteome Discoverer 1.3 version 1.3.0.339. Spectra were searched with OMSSA version 2.1.8 and X!Tandem (Cyclone version 2010.12.01.1) using SearchGUI version 1.10.4 (5) and Peptide Shaker version 0.18.3 (6) against the UniprotKB/SwissProt (reviewed) *Homo sapiens* database, including isoforms with the sequence of porcine trypsin and bovine cytochrome C appended (2012.04.24; 36,275 sequences). Peptide Shaker was used for data validation. Only proteins, peptides, and peptide-spectrum matches with an false discovery rate ≤1% were considered.

The following database search settings were used: MS tolerance of ±10 ppm, CID MS^2 tolerance of 0.5 Da, HCD MS^2 tolerance of 0.02 Da, peptide charge state of 2–4, and enzyme specificity of no enzyme. Oxidations on proline and methionine residues were set as variable modifications; carbamidomethylation

was set as a fixed modification for all database searches. For samples processed with cyanogen bromide, modifications of the C-terminal methionine to homoserine or homoserine lactone were set as additional variable modifications. For samples incubated with formaldehyde/sodium cyanoborohydride, dimethylations on lysine and peptide N-termini were set as variable modifications.

Western Blot Analysis. Proteins were separated by SDS/PAGE under reducing conditions and transferred onto PVDF membranes by semidry or tank electroblotting. Immunodetection was performed using specific polyclonal antibodies raised against epitopes within the procollagen α1(I) [N-propeptide (LF-39), C-propeptide (LF-41), and C-telopeptide (LF-68)] (7). Because the antibody against the N-propeptide does not cross-react with murine collagen α_1(I) N-propeptides, this antibody was not used for the in vivo analyses. Western blots were quantified using ImageJ 1.47.

De Novo Fibril Formation Assay Using Procollagen I Heterotrimers. For transmission electron microscopy, 0.1 mg/mL recombinant procollagen was incubated with 15 nM recombinant proteinase and equimolar PCPE-1 for 60 min at 37 °C in reaction buffer [20 mM Hepes (pH 7.4) and 150 mM NaCl]. Samples were then negatively stained on continuous carbon-coated cupper grids (Science Service) using 2% uranyl formate. Samples (5 μL) were applied to previously negatively glow-discharged grids, washed twice in 20 μL of H_2O, and then placed on an even surface of stain for 2 min. After air-drying, samples were transferred to a Tecnai12 electron microscope operating a LaB6 electron source (FEI). Images were obtained with a 4k × 4k CCD camera (TVIPS).

Experimental Animals. This study used a total of 48 12- to 16-wk-old male mice on a congenic C57BL/6 background. Three genotypes were studied: WT mice and *Mep1a*$^{-/-}$ and *Mep1b*$^{-/-}$ mice in which the meprin genes were ablated (8). Mice were maintained on a 12-h light–dark cycle, with food and water ad libitum.

Isolation of Murine Primary Fibroblasts. Skin biopsy specimens from 6-wk-old *Mep1a*$^{-/-}$, *Mep1b*$^{-/-}$, and WT mice were excised, cut into small pieces using a sterile scalpel, and rinsed in 70% ethanol. After incubation in 0.05% trypsin (Invitrogen) for 1 h at 37 °C, the pieces were transferred onto FCS-coated 25-cm^2 cell culture flasks (Nunc; Thermo Scientific) and covered with DMEM (Invitrogen) supplemented with 10% (vol/vol) FCS and 50 μg/mL gentamycin for 48 h until the first cells adhered. The medium was changed after 48 h and cells were cultured until confluency.

Skin and Cell Lysate Preparation and Protein Determination. Dorsal skin was shaved, dissected, and pulverized into powder in a liquid nitrogen-cooled pestle and mortar. Skin lysates were prepared by adding lysis buffer [50 mM Tris·HCl (pH 6.8), 150 mM NaCl, 1% Triton X100, 1% SDS, and 2 mM EDTA] containing a mixture of complete protease inhibitors (Roche Applied Science) for 24 h at 4 °C. Skin homogenates were then centrifuged at 10,000 × *g* for 30 min at 4 °C. The supernatant was used for Western blot analysis.

For the preparation of cell lysates, cells of passage 8–10 were grown in six-well cell culture plates (Nunc; Thermo Scientific) to 90% confluence. After three washes in PBS, cells were harvested and incubated with lysis buffer as described previously. Protein concentrations were determined using the Bradford protein assay (Roth) with BSA as the standard.

Tissue Preparation for Transmission Electron Microscopy of Dermal Fibrils. Skin samples from age-matched WT, *Mep1a*$^{-/-}$, and *Mep1b*$^{-/-}$ animals were fixed with 2.5% glutaraldehyde in 0.1 M cacodylate buffer (pH 7.5) with 0.1 M sucrose, followed by postfixation with 2% osmium tetroxide. After dehydration in a graded series of ethanol solutions (30%, 50%, 70%, 80%, 90%, 95%, and 100%), samples were embedded in Araldite. Ultrathin (50 nm) sections (Ultracut S microtome; Leica Microsystems) were visualized using a Tecnai12 electron microscope operating a LaB6 electron source (FEI). Images were obtained with a 4k × 4k CCD camera (TVIPS). Average diameters (in nanometers) were obtained by measuring fibrils from three WT mice (n = 414), three *Mep1a*$^{-/-}$ mice (n = 598), and three *Mep1b*$^{-/-}$ mice (n = 414). Graphs were plotted using the R 2.13.0 software package.

Biomechanical Testing of Maximum Skin Tensile Strength. Dorsal skin from WT (n = 6) and aged-matched meprin α (n = 6) and meprin β (n = 6) KO mice was carefully shaved, dissected, and pinned to avoid shrinking. All biopsy specimens tested (three or four per mouse and strain) had a defined hourglass form with a width of 3 mm at the narrowest part, constituting a predefined breaking point. All skin specimens were orientated parallel to the spine and were kept moist with 0.9% isotone NaCl (Braun) at room temperature.

Specimens were held between the gripping jaws and were stretched at a constant rate of 3 mm/s, which resulted in load onset rates of <0.05 N/s. The endpoint was the ultimate load (in Newtons) at which skin disruption occurred. A position encoder (WA300) was used to register the distance covered, and a force transducer for traction and compression (S2; maximum value, 500 N) was used to quantify the power impacting on the skin. The resulting values were recorded by a multiple channel PC measuring device (Spider 8) and plotted as a distance-power curve (Catman 3.0; both from HBM Hottinger Baldwin Messtechnik). The mean maximum tensile strength for each mouse was obtained by averaging three to four measurements per animal.

Histological Studies. Biopsy specimens of dorsal skin of WT (n = 6), *Mep1a*$^{-/-}$ (n = 6), and *Mep1b*$^{-/-}$ (n = 6) mice were fixed for 24–48 h in neutral buffered formalin (4%). After dehydration and embedding in paraffin (Shandon Excelsior ES Tissue Processor; Thermo Scientific), samples were cut into 5-μm sections (Jung SM 2000 R Microtome; Leica Microsystems). Azan trichrome staining was used for visualization of collagen organization. The thickness of the collagen layer was measured by light microscopy (Axiophot; Zeiss) using the morphometry software Diskus 4.8 (Hilgers). The mean thickness of the different specimens was obtained by taking the average of five measurements per section.

RNA Isolation, Reverse Transcriptase-PCR, and Quantitative Real-Time PCR. Total RNA was isolated from skin and primary fibroblasts of WT, *Mep1a*$^{-/-}$, and *Mep1b*$^{-/-}$ mice (n = 3) using the GeneJET RNA Purification Kit (Fermentas, Thermo Scientific). Equal amounts of RNA (1 μg) were transcribed into cDNA in 25-μL reaction mixtures using RevertAid transcriptase (200 U/mL), 10 mM nonspecific oligo d(T) primers, and 200 mM dNTPs (Fermentas, Thermo Scientific). The cDNA obtained was subjected to quantitative real-time PCR measurement in a 10-μL reaction, using the LightCycler480 Real-Time PCR System (Roche Applied Science) according to the manufacturer's instructions. The amplification reaction consisted of a hold of 10 min at 95 °C, followed by 45 cycles of 10 s at 95 °C and 30 s at 60 °C). For assay design, the Universal ProbeLybrary System (http://qpcr.probefinder.com/roche3.html) was used to amplify intron spanning regions for the gene of interest. Relative amounts of target gene mRNA were normalized to the housekeeping gene GAPDH. The following primers/probes were used:

BMP-1/mTLD_forward: gcactatgcccggaacac

BMP-1/mTLD_reverse: cctcatacttgggaacaatgg; probe #80

mTLL-1_forward: aaagagtgcacgtgggtgat

mTLL-1_reverse: aacctcaaactcattgaaggcta; probe #72

mTLL-2_forward: catgagaacggacacgactg

mTLL-2_reverse: cctctgcactgctgatcttg; probe #71.

Connective tissue-associated genes were analyzed using a mouse fibrosis PCR array (SA Biosciences) according to the manufacturer's instructions. ΔΔCp values were used to calculate the relative expression for each data point.

Activity of Human Recombinant MMP-1. The activity of MMP-1 was determined using the quenched fluorogenic peptide MOCAc-Pro-Leu-Gly-Leu-A2(Dnp)-Ala-Arg-NH_2 (R&D Systems). For this, 40 ng of human recombinant pro-MMP-1 was activated with 1 mM p-aminophenylmercuric acetate (APMA) for 2 h at 37 °C before or after incubation with 4.5 nM meprin α or meprin β. All activity assays were performed in 50 mM Hepes (pH 7.5) at 37 °C, and the fluorescence was detected over 120 min. Enzyme activity was measured with the Varioskan Flash fluorescent spectrometer (Thermo Scientific), and data were analyzed using SkanIt Software 2.4 for Varioskan Flash. Proteolytic activity was calculated from the emission at 405 nm with excitation at 320 nm.

1. Becker-Pauly C, et al. (2007) The alpha and beta subunits of the metalloprotease meprin are expressed in separate layers of human epidermis, revealing different functions in keratinocyte proliferation and differentiation. *J Invest Dermatol* 127(5): 1115–1125.
2. Becker C, et al. (2003) Differences in the activation mechanism between the alpha and beta subunits of human meprin. *Biol Chem* 384(5):825–831.
3. Blanc G, et al. (2007) Insights into how CUB domains can exert specific functions while sharing a common fold: Conserved and specific features of the CUB1 domain contribute to the molecular basis of procollagen C-proteinase enhancer-1 activity. *J Biol Chem* 282(23):16924–16933.
4. McQuibban GA, et al. (2002) Matrix metalloproteinase processing of monocyte chemoattractant proteins generates CC chemokine receptor antagonists with anti-inflammatory properties in vivo. *Blood* 100(4):1160–1167.
5. Vaudel M, Barsnes H, Berven FS, Sickmann A, Martens L (2011) SearchGUI: An open-source graphical user interface for simultaneous OMSSA and X!Tandem searches. *Proteomics* 11(5):996–999.
6. Barsnes H, et al. (2011) compomics-utilities: An open-source Java library for computational proteomics. *BMC Bioinformatics* 12:70.
7. Fisher LW, Stubbs JT, 3rd, Young MF (1995) Antisera and cDNA probes to human and certain animal model bone matrix noncollagenous proteins. *Acta Orthop Scand Suppl* 266:61–65.
8. Yura RE, Bradley SG, Ramesh G, Reeves WB, Bond JS (2009) Meprin A metalloproteases enhance renal damage and bladder inflammation after LPS challenge. *Am J Physiol Renal Physiol* 296(1):F135–F144.

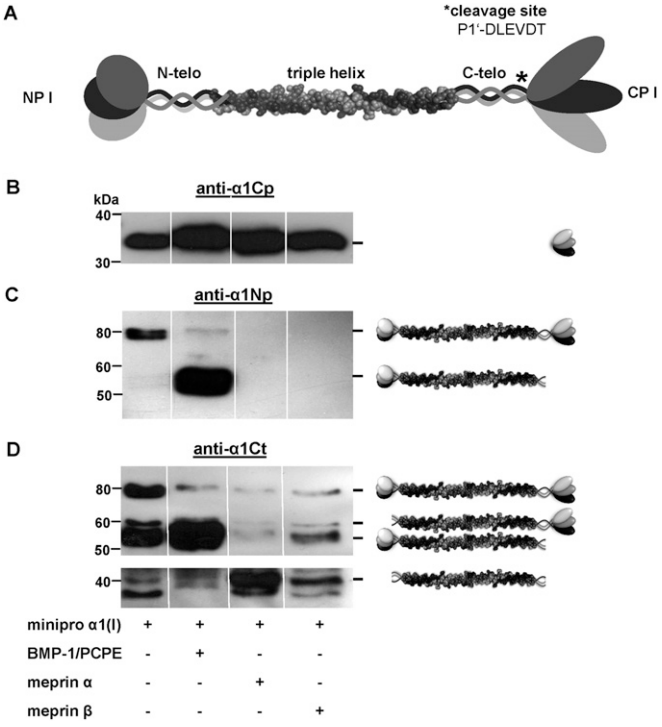

Fig. S1. Cleavage of miniprocollagen α1(I) homotrimer by meprin α and meprin β. (*A*) Schematic of miniprocollagen α1(I) consisting of an N-terminal propeptide (NP), the N-telopeptide (N-telo), the triple helical region, the C-telopeptide (C-telo), and the C-terminal propeptide (CP). The asterisk indicates the cleavage site identified for meprin β by Edman sequencing. (*B–D*) Cleavage of recombinant miniprocollagen I by BMP-1, meprin α, and meprin β. For this, 40 nM miniprocollagen α1(I) was incubated with 0.3 nM BMP-1 and 40 nm PCPE-1, meprin α, or meprin β in a total volume of 50 μL for 60 min at 37 °C in assay buffer. Samples were then analyzed by SDS/PAGE (10% wt/vol polyacrylamide) under reducing conditions, followed by Western blot analysis using anti-collagen α1(I) C-propeptide antibody (anti-α1Cp) (*B*), anti-collagen α1(I) N-propeptide antibody (anti-α1Np) (*C*), and anti-collagen α1(I) C-telopeptide antibody (anti-α1Ct) (*D*).

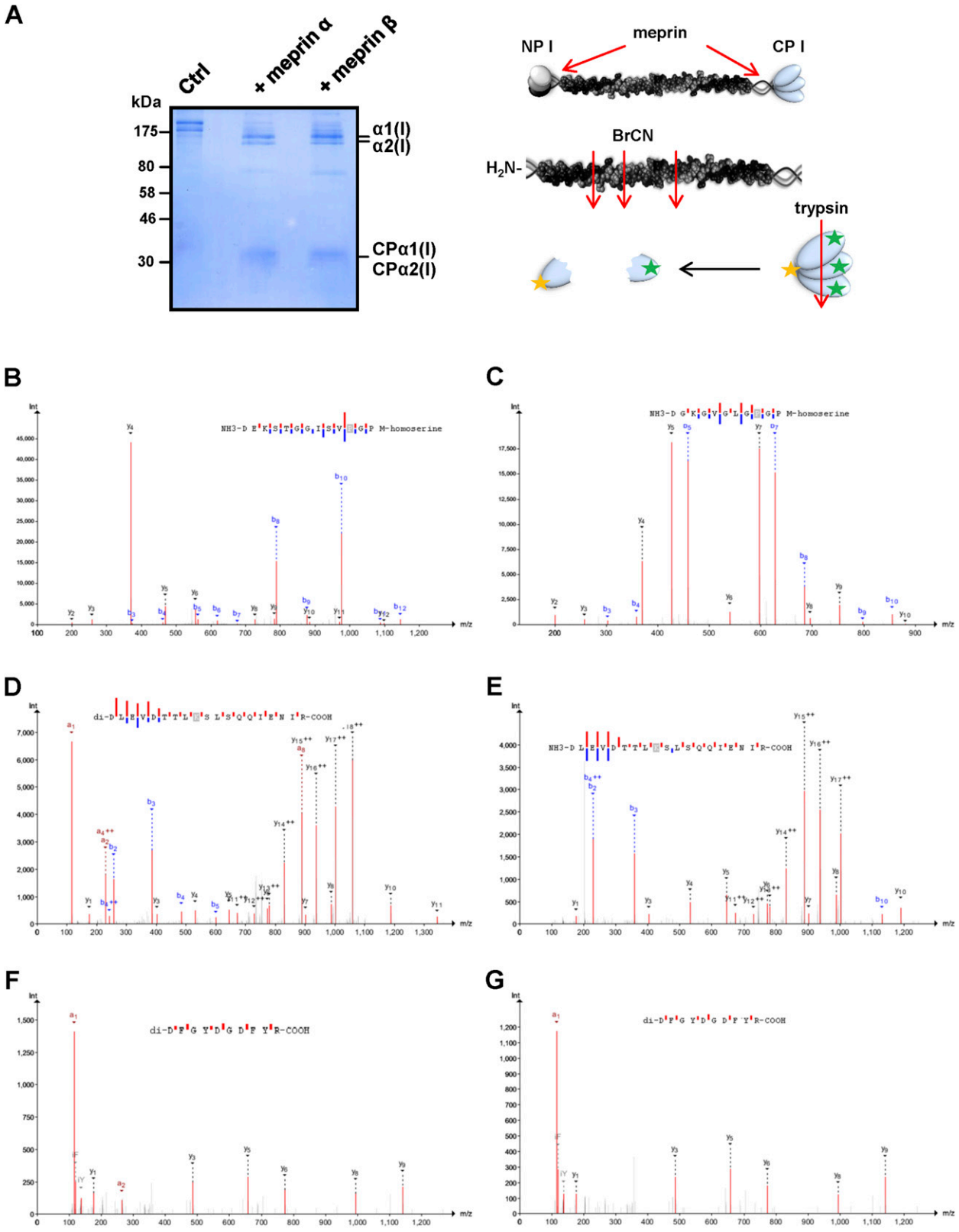

Fig. S2. Proteomic identification of meprin cleavage sites in procollagen I. (*A*) Assignment of the gel bands investigated. The gel is identical to that shown in Fig. 1*C*. N-propeptide cleavage sites in processed procollagen I α1 and α2, by either meprin α or meprin β, were identified by in-gel cyanogen bromide (BrCN) cleavage, followed by nano-LC-MS analysis. C-propeptide cleavage sites of procollagen I α1 and α2 were determined indirectly by identification of the neo-N terminus of the C-propeptides (blue) generated by meprin α or meprin β [CPα1/2(I)]. For this purpose, all free amino groups [neo-N terminus (orange asterisk) and lysine side chains (green asterisks)] were reductively methylated before tryptic in-gel digestion. After cleavage with trypsin, only the N terminus of the cleaved-off C-propeptide was dimethylated (orange asterisk), and thus could be readily identified by LC-MS/MS analysis. (*B*) MS2 CID spectrum of Y(167)/(168)

Legend continued on following page

DEKSTGGISVPGPM, the N-terminal peptide from procollagen α1(I), after treatment with meprin α and subsequent digestion with BrCN. (*C*) MS2 CID spectrum of Y(81)/(82)DGKGVGLGPGPM, the N-terminal peptide of procollagen α2(I) chain, treated with meprin α and then digested with BrCN. Peptides were exported directly from Peptide Shaker version 0.18.3 without further modification. For clarity, satellite signals assigned to loss of water or ammonia are not shown. Proline hydroxylation and modification of the C terminus to homoserine (BrCN-specific cleavage) are indicated. (*D*) HCD MS2 spectrum of R(1227)/(1228) DLEVDTTLKSLQQIENIR from the C-propeptide of the procollagen α1(I) chain released by incubation with meprin α or meprin β. Both lysine and the N terminus are dimethylated. Along with a mass shift of +28 Da, an intense a1 ion is seen, along with the corresponding yn-1 ion ($y182^{+}$), which is characteristic of N-terminal modified peptides. This peptide was not observed in procollagen α1(I) without meprin (see *B*). (*E*) After reductive dimethylation and tryptic digestion of unprocessed procollagen, only the lysine was modified; that is, the peptide is a tryptic peptide. For clarity, loss of water and ammonia ions is not shown. (*F* and *G*) HCD MS2 spectra of peptide Y(1108)/(1109)DFGYDGDFYR from the C-propeptide of the procollagen α2(I) chain released by either meprin α (*F*) or meprin β (*G*). Peptides are N-terminal dimethylated, clearly indicating the neo-N terminus generated from procollagen after meprin cleavage. Peptides were exported directly from the Peptide Shaker without further modification.

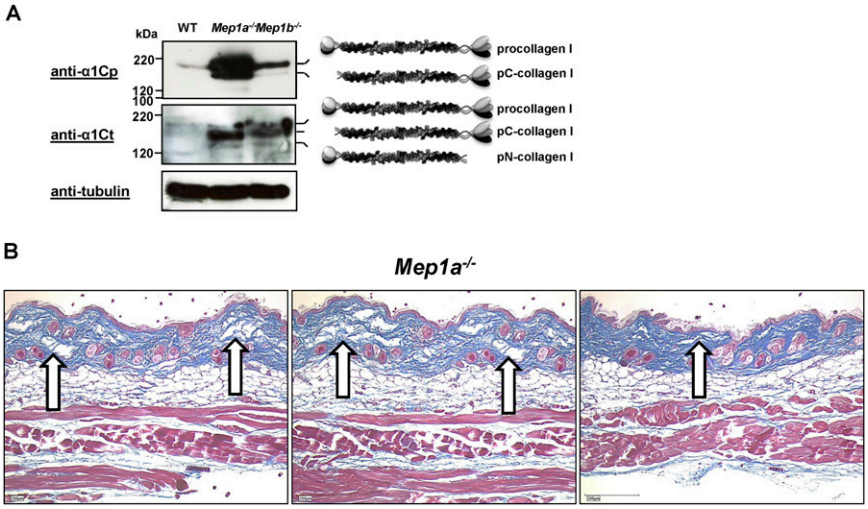

Fig. S3. Processing of procollagen I in primary murine fibroblasts and skin rupture in meprin- deficient skin. (*A*) Western blot analysis of cell lysates prepared from primary murine fibroblasts isolated from WT, *Mep1a*$^{-/-}$, and *Mep1b*$^{-/-}$ mice using antibodies against the collagen α1(I) C-propeptide (anti-α1Cp) or C-telopeptide (anti-α1Ct) with tubulin as the control (anti-tubulin), demonstrating the proteolytic processing of procollagen I in cellulo. (*B*) Azan staining of *Mep1a*$^{-/-}$ skin. Shown is an example of ruptured *Mep1a*$^{-/-}$ tissue caused by section preparation. Arrows point to the breaks in the dermal tissue.

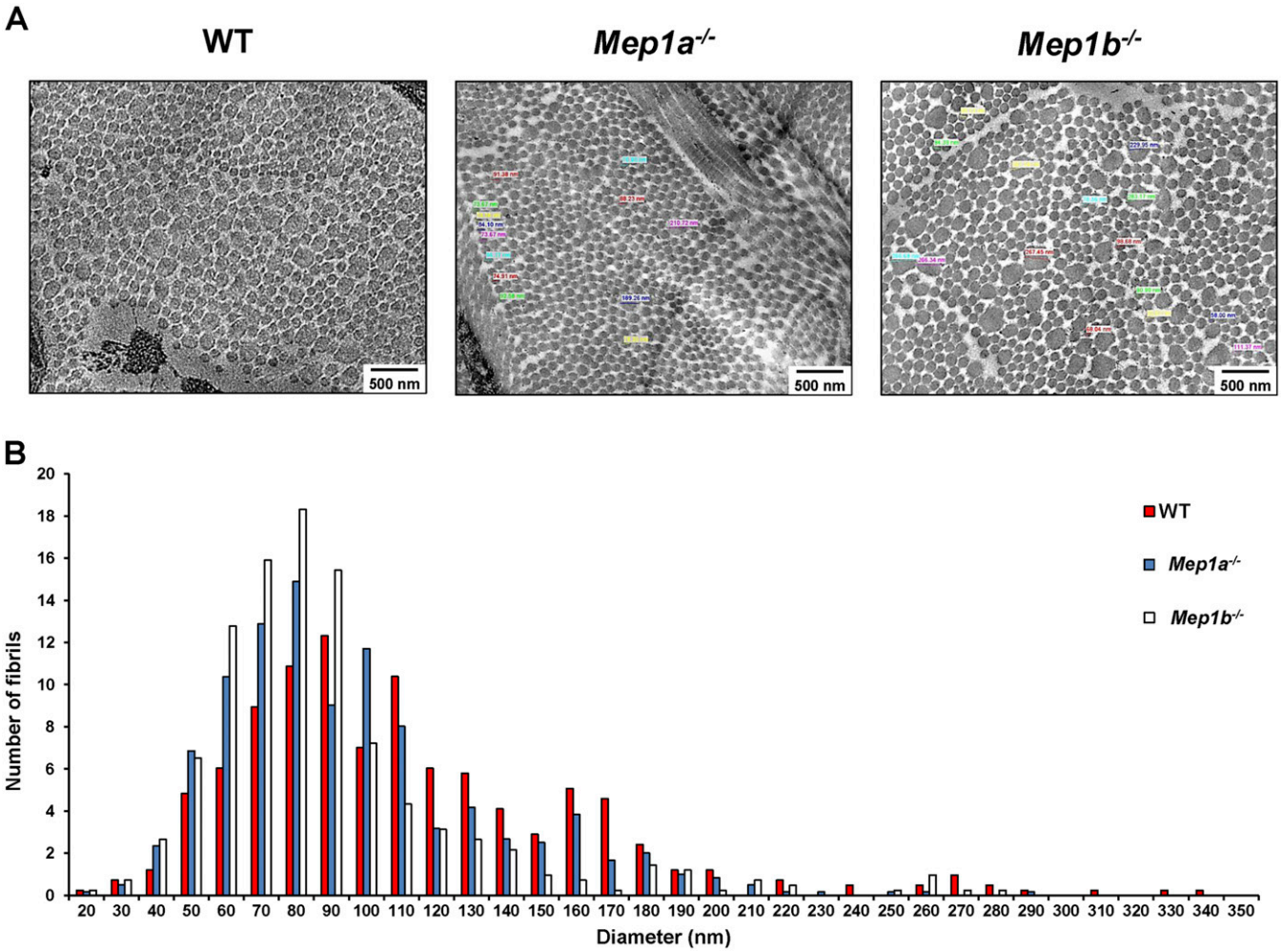

Fig. S4. Disruption of skin tissue and determination of dermal fibril diameter. (*A*) Diameters of the dermal collagen fibrils of *Mep1a*$^{-/-}$ and *Mep1b*$^{-/-}$ mice were determined using Tecnai 12 software (FEI). (*B*) Distribution of dermal fibril diameters of WT, *Mep1a*$^{-/-}$, and *Mep1b*$^{-/-}$ mice, obtained by measuring 414 fibrils from three WT mice, 598 fibrils from three *Mep1a*$^{-/-}$ mice, and 414 fibrils from three *Mep1b*$^{-/-}$ mice.

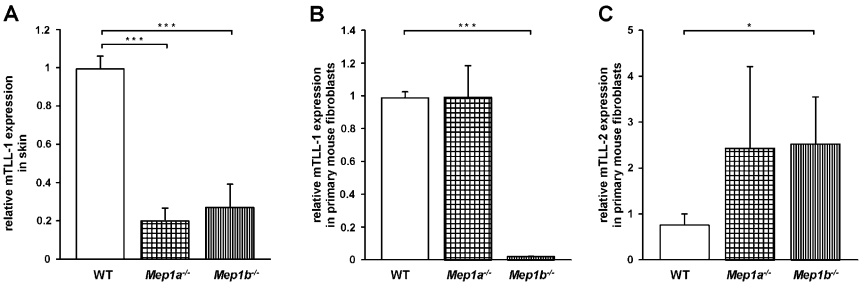

Fig. S5. mRNA expression of the procollagen proteinases mTLL-1 and mTLL-2 is altered in *Mep1a*$^{-/-}$ and *Mep1b*$^{-/-}$ mice. (*A*) Relative expression of mTLL-1 mRNA in the skin of *Mep1a*$^{-/-}$ and *Mep1b*$^{-/-}$ mice analyzed by quantitative real-time PCR. (*B* and *C*) Expression of mTLL-1 (*B*) and mTLL-2 (*C*) analyzed in primary fibroblasts isolated from the skin of *Mep1a*$^{-/-}$ and *Mep1b*$^{-/-}$ mice compared with WT control fibroblasts. $n = 3$. *$P < 0.05$; **$P < 0.01$; ***$P < 0.001$. Error bars show SD.

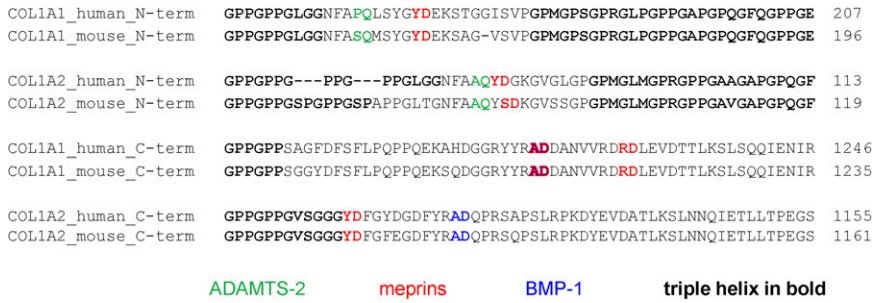

Fig. S6. N-terminal and C-terminal amino acid sequences of human and mouse proα1(I) and proα2(I) chains showing parts of the triple-helical regions and cleavage sites identified for a disintegrin and metalloproteinase with thrombospondin motifs (ADAMTS)-2, BMP-1, and meprins.